PAPER

Direct evidence of traps controlling the carriers transport in SnO_2 nanobelts

Direct evidence of traps controlling the carriers transport in SnO_2 nanobelts

Olivia M. Berengue[1, †] and Adenilson J. Chiquito[2]

[1]LCCTnano, Departamento de Física e Química - Universidade Estadual Paulista (Unesp), Faculdade de Engenharia de Guaratinguetá, Câmpus Guaratinguetá, São Paulo, Brasil

[2]NanO LaB - Departamento de Física, Universidade Federal de São Carlos, CEP 13565-905, CP 676, São Carlos, São Paulo, Brasil

Abstract: This work reports on direct evidence of localized states in undoped SnO_2 nanobelts. Effects of disorder and electron localization were observed in Schottky barrier dependence on the temperature and in thermally stimulated currents. A transition from thermal activation to hopping transport mechanisms was also observed. The energy levels found by thermally stimulated current experiments were in close agreement with transport data confirming the role of localization in determining the properties of devices.

Key words: trap; transport; SnO_2

DOI: 10.1088/1674-4926/38/12/122001 **EEACC:** 2520

1. Introduction

Quasi 1D metal oxide nanostructures have attracted considerable interest in recent years for fundamental studies and also for potential applications. In particular, they present properties which range from metals to semiconductors and insulators. One of the most prominent applications of these materials is the gas sensing devices[1–5]. The large surface-to-volume ratio inherent in one-dimensional nanostructures, provides the basis for superior sensor function by the oxide devices. On the other hand, it is well known that the performance of these devices is strongly correlated to their structural and electronic properties and to the presence of defects that limit the long-term reliability tolerance of electronic materials and devices. The understanding and the eventual control of these deleterious effects is of great relevance in view of device applications. SnO_2 is an intrinsic n-type semiconductor (mostly induced by oxygen vacancies) usually found in a rutile structure[6]. The coexistence of low resistivity and optical transparency is a characteristic feature of this class of materials but the electrical conductivity is unstable due to the reaction of oxygen vacancies in the SnO_2 and the environment atmosphere. In fact, this feature makes SnO_2 an excellent material for gas sensing devices either as thin films or as nanowires and nanobelts[7].

The physical principles underlying the detecting (gas and light) properties of semiconducting metal oxides have been explained elsewhere[5]: due to the affinity of O_2 molecules and the metal oxide nanostructures the molecules can be adsorbed on the surface of the nanowire, reacting with nearby electrons and thus, reducing the density of free electrons. In this way, the conductivity of the structures is reduced. By applying light (in the ultra-violet range), the original conductance is recovered: electron-hole pairs are formed and the holes recombine with the O_2^- bringing the structure to the original state. The actual sensor/device technologies consider that the transport in nanowires is dominated by a diffusive regime in which the undepleted region (far away from interfaces) responds in the ohmic regime. However, the conductivity in these one-dimensional devices is decisively affected by surface states and external excitations such as light and the surrounding environment. The surface disorder produced during the synthesis randomizes the electronic potential near the surface and then electrons are subjected to localization. This disorder can be described by surface states which affect all electrical properties of metal-nanowire devices. The fact is that any electron subjected to a random potential is not able to move through the system if either potential fluctuations exceed a critical value or the electron energy is lower than the characteristic value of the potential fluctuations. One of the common consequences of the localization is the hopping transport mechanism found in nanowire devices[8]. This work reports on direct evidence of localized states in undoped SnO_2 nanobelts synthesized from vapor-solid mechanism. From current-voltage measurements in back-to-back Schottky diodes we found a temperature dependence of the barrier height. This is a sign of charge localization at the metal-semiconductor interfaces and in regions nearby. Also, hopping transport was identified in a broad range of temperatures (low temperatures) while Arrhenius excitation was observed in high temperatures. The strength of electron's localization was studied by thermally stimulated current measurements (TSC). This method is broadly used for determining trapping parameters in semiconductors[9]. We found two energy levels which are in agreement with the hopping and activation mechanisms observation.

2. Experimental

Tin oxide nanobelts were synthesized in a conventional horizontal tube furnace (Lindberg Blue M) where it was inserted a ceramic alumina tube loaded with a powder mixture of

† Corresponding author. Email: oliberengue@gmail.com

Received 2 January 2017, revised manuscript received 16 June 2017

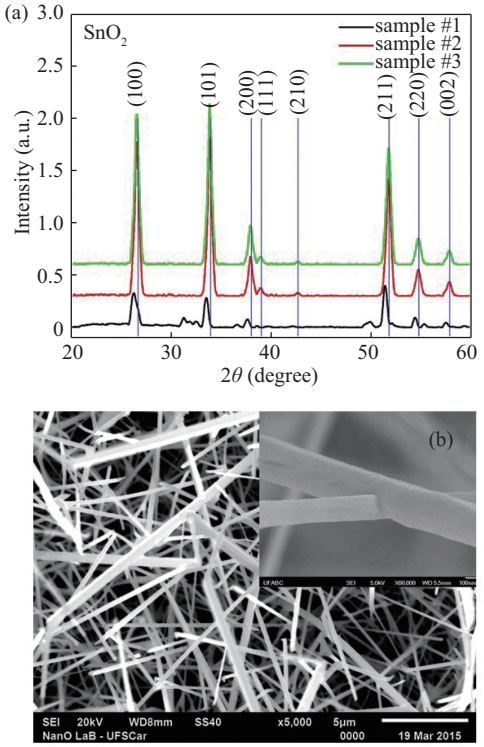

Fig. 1. (Color online) (a) XRD data for three different as-grown samples showing the rutile-like peaks (PDF 41-1445) expected for the tetragonal SnO_2 structure. Panel (b) shows an SEM image of the as-synthesized nanostructures. We found belts with lateral sizes ranging from 50 to 400 nm and lengths of tens of micrometers and also wires with sizes ranging from 30 to 300 nm and lengths of tens of micrometers. Also, in the inset there is a large magnification image showing the cross-section of the nanobelts in detail.

SnO_2 (Sigma Aldrich, purity > 99.99%) and carbon black (Union Carbide, purity > 99.99%) mixed in a homemade balls mill. Previously to the heating process, the tube was purged with a 200 sccm nitrogen gas flux in order to avoid undesirable presence of oxygen before the powder reaches the ideal temperature for the synthesis (1200 °C). Afterwards, the flow rate was adjusted to 60 sccm. The furnace was rapidly heated to 450 °C (heating rate of 10 °C/min) and oxygen traces were inserted in order to both drive the source material to the coldest region of the tube and to avoid non-stoichiometric SnO_2 phases[10].

The as-grown materials were characterized by X-ray diffraction (Shimadzu, XRD 6100, 40 kV, 30 mA, Cu Kα radiation; all measurements were performed by using aluminium sample holders) and scanning electron microscopy (SEM, Jeol JSM6510) and the results can be seen in Figs. 1(a) and 1(b), respectively. The XRD data presented in panel (a) from the as-grown material show rutile-like peaks (PDF 41-1445) expected for the tetragonal SnO_2 structure.

All diffraction peaks were indexed as the tetragonal structure of SnO_2 within the P42/mnm spatial group (JCPDS card number 41-1445) and no additional phase peak was observed. The intensity ratio between reflections [110] and [101], $I_{(110)}/I_{(101)} = 0.96$ provides an indication of a preferential orientation growth, when compared with the standard data ($I_{(110)}/I_{(101)}$). The difference is related to the large aspect ratio of the morphology of those samples.

Fig. 1(b) shows an SEM image of the synthesized samples. We found belts with lateral sizes ranging from 50 to 400 nm and lengths of tens of micrometers and also wires with sizes ranging from 30 to 300 nm and lengths of tens of micrometers. Also, in the inset there is a large magnification image showing the cross-section of the nanobelts in detail.

The production of the one-nanobelt-based devices started with the deposition of the SnO_2 samples onto the SiO_2 (500 nm thick) substrates before the definition of the metallic patterns: 500 nm thick titanium for Schottky devices and 80 nm thick eutectic alloy of Au/Ni for ohmic contacts. The metallic patterns were defined on nanobelts by standard photolithography techniques and in such a way that after the lift-off process only one nanobelt is linked by two metallic contacts. After this process, devices were inserted in adequate sample holders in order to perform electrical measurements. For TSC measurements, we used the following procedure: unbiased samples were cold down at 8 K in a closed cycle helium cryostat (Janis Research, CCS 400 H) at pressures below 10^{-6} mbar; at the temperature minimum, samples were irradiated with the ultra-violet light and the temperature was increased at a constant rate (4 K/min) recording the thermally generated currents. Our system was able to determine currents lower than 10^{-15} A. Thermally stimulated currents were monitored using a Keithley 6517B electrometer; the ultra-violet light was produced by a mercury lamp with 20 W of nominal power.

3. Results and discussion

Current-voltage curves are displayed in Fig. 2(a) for a single nanobelt device at different temperatures. Although the metal used for the two contacts is the same, the electrical characteristics are clearly distinct (asymmetry). This is a consequence of different Schottky barriers at each interface and a first evidence of the effects caused by potential fluctuations due to disorder. This disorder, directly contributes to the whole electron transport process in the samples. Using the back-to-back model in order to fit these current–voltage curves, we were able to find the Schottky barriers at both interfaces [Fig. 2(b)]. These Schottky barrier values are very different from those found in literature, $\phi_B = 0.4$–0.42 eV[11, 12] and they should be related to the influence of an interface layer where charges are localized. Under the growth conditions some disorder is expected to appear at the nanobelt's surface. Therefore it is reasonable to assume that the irregularities on the surface should induce some inhomogeneity of the Schottky barrier height. This inhomogeneity, in turn, implies a temperature dependence of the Schottky barrier due to the different occupation of the energy levels at the interface under the Schottky barrier. Then an apparent distribution of Schottky barriers is seen in a typical measurement: different levels are activated at distinct temperatures as observed in Fig. 2(b).

For a barrier distribution, ϕ_B can be obtained from[13]

$$\phi_B = \phi_{B0} + \frac{\sigma^2}{2k_B T}, \quad (1)$$

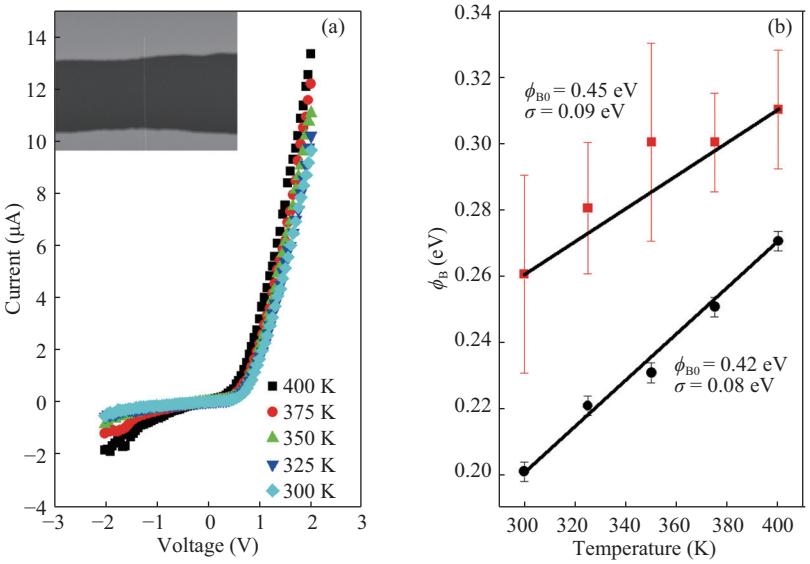

Fig. 2. (Color online) Current–voltage curves for a single nanobelt device at different temperatures. Although the metal used for the two contacts is the same, the electrical characteristics are clearly distinct (asymmetry). Using the back-to-back model in order to fit these current-voltage curves, we found Schottky barriers at both interfaces as depicted in panel (b).

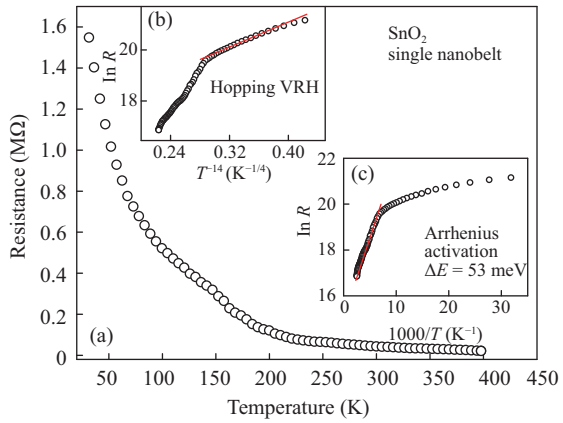

Fig. 3. (Color online) Resistivity of SnO_2 devices decreased as the temperature increased as should be expected for semiconductors, panel (a). Panels (b) and (c) show regions where variable range-hopping mechanism and Arrhenius-type mechanisms were found, respectively.

where ϕ_{B0} is the correct Schottky barrier, σ^2 is the standard deviation of the barriers distribution and the other symbols have their usual meanings. The lines in Fig. 2(b) represent the fitting of Eq. (1) to the experimental data: we found ϕ_{B0} = 0.42 eV and ϕ_{B0} = 0.45 eV in close agreement with literature data[11]. The consideration of the contributions from disorder and localization of charges are very important in order to understand the behavior of the devices. This dependence of the Schottky barriers on the temperature is an indirect evidence of the disorder effects.

The effects of the disorder can also be identified in transport measurements (Fig. 3). The resistivity of SnO_2 devices decreased as the temperature increased as should be expected for semiconductors [Fig. 3(a)] and shows two regions where a variable range-hopping mechanism and an Arrhenius-type mechanism can be observed as displayed in Figs. 3(b), 3(c), respectively. From the high-temperature range (T > 130 K) the activation energy was extracted out to be $\Delta E = 53 \pm 10$ meV in good agreement with literature data[14]. In the low-temperature range the electric transport is dominated by a hopping process. As mentioned above, vacancies provide carriers for the n-type character of the undoped SnO_2 but also they are a natural source of disorder that randomizes the local electronic potential leading to localization. The transport in these disordered systems is then characterized by hopping between the localized states as pointed out by Mott[15] and described by

$$\rho(T) = \rho_0 \exp\left(\frac{T_0}{T}\right)^{\frac{1}{4}}, \qquad (2)$$

where $T_0 = \frac{18\alpha^3}{k_B N(E_F)}$, $N(E_F)$ is the density of states at the Fermi level and α^{-1} the localization length characterizing the spatial extension of wave functions. The conduction takes place by hopping in the vicinity (around k_BT) of the Fermi level where the density of states remains almost a constant. This condition is fulfilled when the temperature is sufficiently small or when the energy states are uniformly distributed. The agreement between theoretical and experimental curves confirms that the hopping process governs the transport from 10 to 130 K. In fact fitting of Eq. (2) to the experimental data provides $N(E_F) = 6.8 \times 10^{20}$ eV^{-1}cm^{-3} when considering that $\alpha = (a_B)^{-1}$ where a_B is the Bohr radius of SnO_2 ($m^* = 0.24m_0$). The average hopping energy was calculated to be 12 ± 8 meV at 130 K (temperature in which thermal activation starts to be significant).

The presence of localized states can be extracted out directly from thermally stimulated current measurements which is a broadly used method for determining trapping parameters in semiconductors. In typical TSC measurement, samples are irradiated with UV light and cooled to 8 K, thus stimulating carriers trapped in deep levels lying in the forbidden energy gap[16]. If there is an electron trapping centre with energy above the normal dark Fermi level, then trapped elec-

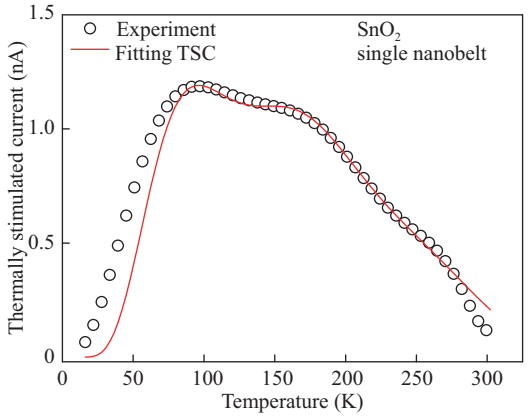

Fig. 4. (Color online) Thermally stimulated current measured in a single nanobelt device showing two different levels at 100 and 190 K. The energies for these levels were found to be 16 and 51 meV.

trons will be in a non-equilibrium state, thereby their rate of release will depend mainly on the phonon energy available in the lattice. Thus, after removing the optical stimulation the traps will empty into the conduction band with the rise of temperature, producing temporary increases in the electric current. As the number of filled traps diminishes with time and there is no injection due to the Schottky barrier, the excess conductivity presents maximum points. Being a displacement current, TSC is sensitive to both number of charges moving within a system and distances travelled by them. The TSC method is generally used to estimate energy distributions of defects as opposed to densities[17]. Fig. 4 shows the thermally stimulated currents measured in a single nanobelt device. The peaked character of the curve is evidence that trapping processes are present in the samples. The thermally generated current is quantitatively written as

$$I_{\mathrm{TSC}}(T) = I_0 \exp\left[\frac{-\Delta E}{k_{\mathrm{B}}T} - \frac{1}{N_{\mathrm{T}}\beta\tau}\int_{\mathrm{T_0}}^{T} N_{\mathrm{C}} \exp\left(\frac{-\Delta E}{k_{\mathrm{B}}T}\right)\mathrm{d}T\right], \quad (3)$$

where N_{C} is the electron density of states, N_{T} is the density of the localized electrons, ΔE is the activation energy necessary to release trapped carriers, β is the heating rate, T_0 is the trap filling temperature and and τ is the carrier recombination lifetime. The excitation energies of localized electrons were obtained by fitting of Eq. (3) to the experimental data.

The agreement between theoretical and experimental points is quite remarkable in the whole range of temperatures (10 K < T < 300 K). This result shows the presence of levels at 16 ± 5 meV and 51 ± 8 meV, confirming the presence of localization and its relationship with the observed transport features: these energies are close to those found from transport measurements, indicating that the disorder randomizes the electron potential leading to localization. The hopping energy at low temperatures is close to the lower energy found in TSC experiments while the activation energy (Arrhenius) is close to the higher energy level also found in TSC.

4. Conclusion

Single nanobelt-based devices with Ti electrodes were constructed in order to investigate defects and disorder's influence on electrical properties. Schottky contact properties were studied using a model which considers a back-to-back Schottky barrier and we found a dependence of the barrier height on the temperature indicating the presence of localized states. Transport data reveals two distinct transport mechanisms present in the samples: VRH hopping and Arrhenius-type were detected in different temperature ranges. Also, the activation energy was extracted out from the Arrhenius data to be 53 ± 10 meV as well as the average hopping energy was calculated to be 12 ± 8 meV. Thermally stimulated measurements show the presence of two energy levels, 16 ± 5 meV and 51 ± 8 meV which present good agreement with the transport data and also confirm the presence of localization in SnO_2 samples.

Acknowledgments

We thank professor Alexandre J. C. Lanfredi for FEG-SEM image and the Brazilian research funding agencies (Grant 13/19692-0, 15/21816-4 São Paulo Research Foundation (FAPESP)) and CNPq (477716/2013-0) for the financial support of this work.

References

[1] Sberveglieri G, Faglia G, Groppelli S, et al. Ultrasensitive and highly selective gas sensors using three-dimensional tungsten oxide nanowire networks. Semicond Sci Technol, 1990, 5(12): 1231

[2] Göpel W. Ultimate limits in the miniaturization of chemical sensors. Sens Actuators A, 1996, 56(1/2): 83

[3] Henrich V E, Cox P A. The surface science of metal oxides. Cambridge University Press, 1994

[4] Barsan N, Schweizer-Berberich M, Gopel W. Fundamental and practical aspects in the design of nanoscaled SnO_2 gas sensors: a status report. Fresenius J Anal, 1999, 365(4): 287

[5] Kolmakov A, Klenov D O, Lilach Y, et al. Enhanced gas sensing by individual SnO_2 nanowires and nanobelts functionalized with Pd catalyst particles. Nano Lett, 2005, 5(4): 667

[6] Dai Z R, Gole J R, Stout J D, et al. Tin oxide nanowires, nanoribbons, and nanotubes. J Phys Chem B, 2002, 106(6): 1274

[7] Grace Lu J, Chang P, Fan Z. Quasi-one-dimensional metal oxide materials-synthesis, properties and applications. Mater Sci Eng R, 2006, 52(1–3): 49

[8] Lanfredi A J C, Geraldes R R, Berengue O M, et al. Electron transport properties of undoped SnO_2 monocrystals. J Appl Phys, 2009, 105(2): 023708

[9] Berengue O M, Kanashiro M K, Chiquito A J, et al. Detection of oxygen vacancy defect states in oxide nanobelts by using thermally stimulated current spectroscopy. Semicond Sci Technol, 2012, 27(6): 065021

[10] Berengue O M, Simon R A, Chiquito A J, et al. Semiconducting Sn_3O_4 nanobelts: growth and electronic structure. J Appl Phys, 2010, 107(3): 0337171

[11] Korber C, Harvey S P, Mason T O, et al. Barrier heights at the SnO_2/Pt interface: in situ photoemission and electrical properties. Surf Sci, 2008, 602(21): 3246

[12] Wager J F. Transparent electronics: Schottky barrier and heterojunction considerations. Thin Solid Films, 2008, 516(8): 1755

[13] Werner J H, Guttler H H. Barrier inhomogeneities at Schottky contacts. J Appl Phys, 1991, 69(3): 1522

[14] Lai M, Lim J H, Mibeen S, et al. Size-controlled electrochemical synthesis and properties of SnO_2 nanotubes. Nanotechnology, 2009, 20(18): 185602

[15] Mott N F. Metal–insulator transitions. Taylor and Francis, 1990

[16] Wrobel J M, Gubanski A, Placzek-Popko E, et al. Thermally stimulated current in high resistivity $Cd_{0.85}Mn_{0.15}Te$ doped with indium. J Appl Phys, 2008, 103(6): 063720

[17] Wright H C, Allen G A. Thermally stimulated current analysis. J Appl Phys, 1966, 17(9): 1181